

# Regression Analysis of Process Parameters in Photochemical Machining of SS-304

<sup>1,3</sup>Agrawal Devendra, <sup>2</sup> Dinesh Kamble

<sup>1</sup>Research Scholar, <sup>2</sup> Professor, <sup>3</sup>Assistant Professor

<sup>1</sup>Department of Mechanical Engineering, SCOE Vadgaon (Bk.) SPPU Pune India.

<sup>2</sup>Department of Mechanical Engineering, VIIT Pune, SPPU Pune, India.

<sup>3</sup>Department of Mechanical Engineering, SVPM'S COE Malegaon (Bk.) SPPU Pune India.

## Abstract:

Non-traditional machining are showing the prominent application in electronics engineering, micro machining , aerospace applications and now a days in biomedical engineering Photochemical machining (PCM) is used as one of the best micromachining technique for machining of difficult-to-cut material with appropriate machining parameters combination. The ferric chloride is used as etchant for machining of stainless steel-304. In the present work, an effort is made to explore the potentialities of application Regression Analysis (RA) in photochemical machining process. Design of Experiments (DoE) with Full factorial ( $L_{27}$ ) is worked out with machining parameters such as time of etching, temperature of etchant and concentration of etchant on the predominant micromachining criteria like Material Removal Rate (MRR), Surface roughness ( $R_a$ ), Undercut ( $U_c$ ) and Etch Factor (EF). Based on the observations, regression models are derived with acceptable degree of correlation between experimental and regression values. The values of coefficient of regression are showing a good agreement in experimental values and predicted by the regression model with minimum percentage error.

**Index Terms - PCM; Etching; Phototool; Undercut; MRR; Regression analysis;**

## I. INTRODUCTION

Nontraditional machining processes are widely employed to manufacture geometrically complex and high-dimensional accurate machine parts from advance material in industry as diverse as aerospace, electronics and automotives. Various nontraditional machining processes are employed for micro size production in engineering and biomedical field [1]. Photochemical machining (PCM) is a nonconventional machining process employing photoresist and chemical etching technology to produce precision parts [2]. PCM is essentially accelerated and controlled corrosion. When Ferric chloride ( $FeCl_3$ ) is dissolved in water the solution becomes strongly acidic as a result of hydrolysis. Ferric chloride in water solution ionizes to iron ( $Fe^{3+}$ ) and chloride ions. Due to electro-negativity, elements of stainless are combining with ferric ion from the solution. The etching takes place through three steps. In first step the ions or molecules from the etchant solution diffused towards the exposed area on the metal surface through the boundary layer. The second step consists of chemical reaction between etchant and the exposed metal surface results in soluble and gaseous by-product formation. The by-product from the surface of the work piece gets diffused through the boundary layer into the etchant solution in third step. The mechanics of process involves the breaking of covalent bond between different grains of polycrystalline material across the cathode and anode interface i.e. grain boundary. It is performed by doing controlled corrosion at the anodic surface due to chemical reaction between ferric ions and metal grains. This grain boundary has the lowest potential called open circuit potential. Fadaei et al. (2004) have used TEA (triethanolamine) for chemical machining of St304 and result reported good surface finish with high machining rate [3]. Allen et al. aims at defining standards for industrial etchants and methods by which it can be analyzed and controlled [4]. Cakir (2008) introduced the ferric chloride as a suitable etchant for aluminum etching [5]. The versatile aqueous ferric chloride is used for etching of SS-304 [6]. The chemical etching of brass, German silver and Inconel 718 is reported with ferric chloride and cupric chloride as etchant and the effect of etchant and machining condition on the depth of etch and surface roughness is investigated [7,8]. The PCM shows advantages such as finished products are burr free and stress free hence no further treatment is required. The chemical and physical properties of the parts remain unchanged. There is no heat affected areas at the cut edges as observed in laser cutting process or loss of magnetic permeability and stress caused as in stamping process. Low tool cost and short lead time make the machining process excellent for small and medium production and unique manufacturing method for components with extreme complexity [9]. The PCM process have drawback like Undercut ( $U_c$ ) i.e. unwanted machining of substrate material under the photoresist (shown in Figure 2) [10, 11]. Through the literature survey and effect cause analysis, it is observed that the major influencing parameters for the PCM process are time of etching (min.), temperature of etchant ( $^{\circ}C$ ) and concentration of etchant (g/l) [7]. The optimum machining parameters are obtained in PCM of SS-304 to get the best machining outcome under given experimental condition. The optimum machining parameters obtained after Weighted Grey Relational Analysis (WGRA) are concentration of etchant 750 g/l, time of etching 40 min and temperature of etchant  $55^{\circ}C$  [12]. In the current investigation, an attempt is made to predict and analyze the responses obtained after the Design of Experiment (DoE) with the help of Regression Analysis method.

**II. PHOTOCHEMICAL MACHINING PROCESS**

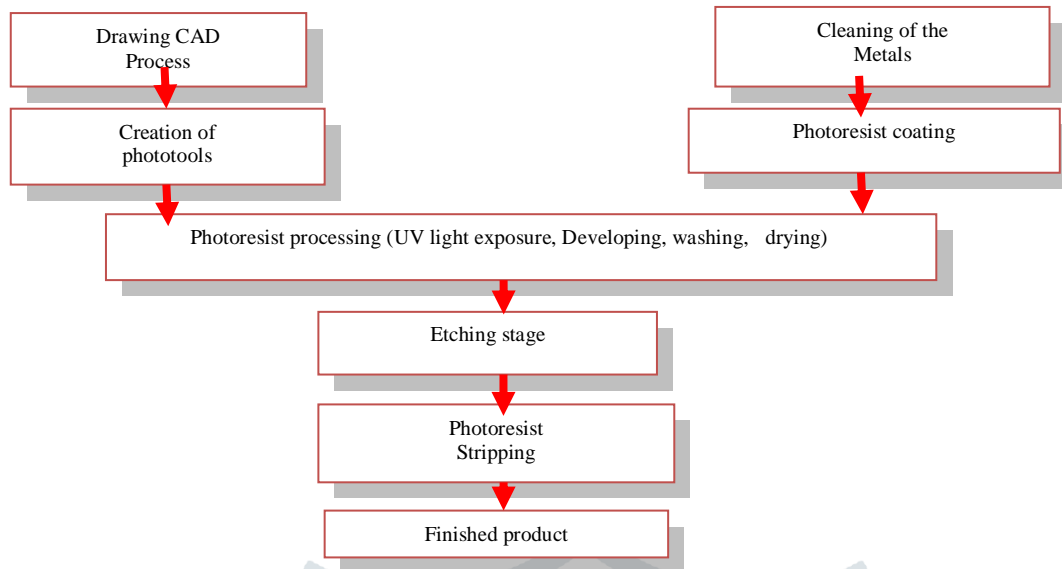


**Fig.1.IPCM Process flow Chart**

**III. EXPERIMENTAL PROCEDURE**

The steps in PCM process are shown in Figure 1. The substrate (SS-304) with size of 30mm x 30mm is cleaned with acetone and water with neutral PH to remove dirt and dust and dipped in the tank of photo resist (LPR, E-1020 Negative type) called as dip coater. The thickness of photoresist coating over the specimen is controlled by centrifugal coating technique [12]. The specimen is rotated with 300 rpm for 10 seconds with photoresist for uniform coating. The photoresist is dried for 10 minutes on specimen in drier. The development of phototool is the important step during the process. The limits for micro machining with PCM process mainly depend on the size of phototool developed. The CorelDraw (CAD) software with accuracy of 1µm is used to develop the size of phototool. The phototool with black circle of size of 10mm diameter is developed on transparent paper using CAD software. The developed phototool is used for performing the L<sub>27</sub> set of experiments. The laser jet or solid ink techniques are used to print the CorelDraw drawing directly on transparent paper. The main governing characteristics of the phototool printed by laser printers are the use of toner particles, comprising binder polymers, colored and charge controlling agents deposited on transparency paper. The dried specimen and phototool are exposed under the U-V light for two minutes. The UV light is used to obtain smaller resolution because of its lower value of wavelength. Specimen is rinsed in developer (LPR developer) to observe the image of phototool on the photoresist. It polymerizes the photoresist under exposure of U-V light by forming the rigid cross link between the monomers which will remain unetched (as mask) during machining. The developer removes the photoresist which is not under the exposure of U-V light and etching will proceed across that area i.e. circle with diameter of 10mm. The experimental set up is shown in Figure 3. The titanium heater is used to increase the temperature of etchant. The temperature of etchant is regulated by thermocouple and measured by infrared thermometer. The compressed air is applied at bottom of etching tank to maintain uniform concentration of etchant. Specimen is placed in the etching tank inside the cage of polymer to avoid the contact with wall of tank. The L<sub>27</sub> array is performed with three sets of replica to avoid experimental and measurement error. Surface roughness (R<sub>a</sub>) is one of the important factors that affect the quality of a machined surface. It is measured by using Mitutoyo surface roughness tester (cutoff length 0.8mm, Filter Gauge, M-speed-0.50 mm/s). Undercut (U<sub>c</sub>) is the difference between the radius of the machined hole and the standard hole size i.e. phototool (Figure 3). The two circles are observed under Video Measuring Machine (VMM) after the removal of photoresist. The larger circle represents the surface with undercut and smaller circle represent the exact sizes of phototool i.e. dimension required (Figure 4). The radius of the hole with undercut is obtained by averaging the ten values of radius marked with VMM on the circumference of the larger circle. The difference between outer and inner radius is selected as the undercut for observed specimen. Material Removal Rate (mm<sup>3</sup>/min.) is calculated by volume of material removed (depth of cut x area under etching) dividing by its respective time (min). Etch Factor obtained by taking ratio of depth of cut to undercut. The response values are calculated by taking the average of readings of three sets of replica for each set of experimentation. The response values after the experimentation are shown in Table 2.

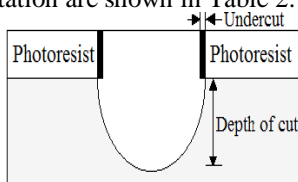


**Fig.2 Undercut**

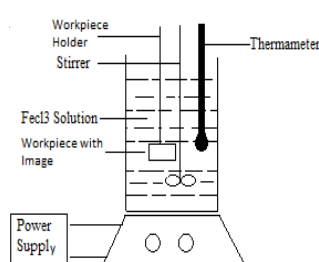


**Fig.3 Experimental setup for controlled etching of specimen**

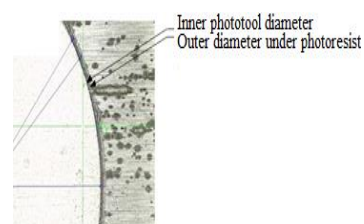


**Fig. 4 Undercut observed under VMM**

### 3.1 Design of Experimentation

During the experimentation, a large number of trials have to be carried out as the number of machining parameters increases. Design of Experiment (DoE) involves proper selection of variables (input factors) and their interactions. The most important stage in the DoE lies in the selection of the control parameters and their levels. The use of spastically derived full factorial design gives the number of experimental runs to be carried out without affecting the quality of analysis. The Full Factorial ( $L_{27}$ ) design method is used for experimentation with machining criteria as larger is better for Material Removal Rate (MRR) and Etch factor (EF) and smaller is better for Surface roughness ( $R_a$ ) and Undercut ( $U_c$ ). The process variables and their levels are primarily selected based on the literature survey [7] and effect cause analysis observed by researcher. The preliminary (pilot) set of experiments are conducted with one factor at a time approach to set the level of machining parameters (shown in Table 1). The levels of machining parameters selected for  $L_{27}$  are the concentration of etchant as 650 g/l, 750 g/l and 850 g/l, time of etching as 30 min., 40 min. and 50 min. and temperature of etchant as 50°C, 60°C and 70°C after preliminary sets experimentation with three replica sets.

**Table 1 :** The levels used for DoE

	Low	Medium	Low
Concentration (g/l.)	650	750	850
Temperature (°C)	50	60	70
Time (min.)	30	40	50

The  $3^k$  full factorial design consists of all combinations of all the k factors taking 3 levels. These are high, medium and low levels of factors. According to the  $3^k$  full factorial design, 27 experiments are planned with three sets of replica [11].

**Table 2:** Response table

Sr.No.	$R_a$ ( $\mu\text{m}$ )	S/N Ratio	$U_c$ (mm)	S/N ratio	MRR ( $\text{mm}^3/\text{min.}$ )	S/N ratio	EF	S/N ratio
1	1.683	-4.5217	0.0270	31.3727	3.140	9.9386	1.48	3.40523
2	0.741	2.6036	0.0473	26.5028	6.044	15.6265	1.62	4.19030
3	0.707	3.0116	0.0623	24.1102	6.280	15.9592	1.52	3.63687
4	1.066	-0.5551	0.0304	30.3425	3.297	10.3624	1.41	2.98438
5	2.287	-7.1853	0.0413	27.6810	4.553	13.1660	1.40	2.92256
6	0.573	4.8369	0.0523	25.6300	7.928	17.9833	1.93	5.71115
7	0.747	2.5336	0.0930	20.6303	7.614	17.6323	1.03	0.25674
8	0.980	0.1755	0.0944	20.5006	7.771	17.8095	1.04	0.34067
9	1.402	-2.9350	0.0573	24.8369	7.928	17.9833	1.76	4.91025
10	0.877	1.1400	0.0677	23.3882	5.338	14.5476	1.00	0.00000
11	1.354	-2.6324	0.0736	22.6624	7.693	17.7219	1.33	2.47703
12	0.970	0.2646	0.0964	20.3185	8.870	18.9585	1.17	1.36372
13	1.155	-1.2516	0.0772	22.2477	6.410	16.1372	1.04	0.34067
14	0.984	0.1401	0.0821	21.7131	7.879	17.9294	1.14	1.13810
15	0.202	13.8930	0.0710	22.9748	8.910	18.9976	1.71	4.65992
16	0.968	0.2825	0.0770	22.2702	6.672	16.4851	1.10	0.82785
17	1.082	-0.6845	0.0725	22.7932	7.457	17.4513	1.31	2.34543
18	2.258	-7.0745	0.0850	21.4116	7.693	17.7219	1.15	1.21396
19	0.864	1.2697	0.0811	21.8196	7.771	17.8095	1.22	1.72720
20	1.006	-0.0520	0.0670	23.4785	5.479	14.7740	1.47	3.34635
21	0.884	1.0710	0.0827	21.6499	8.478	18.5659	1.30	2.27887
22	0.859	1.3201	0.0661	23.5960	5.700	15.1175	1.10	0.82785
23	1.042	-0.3574	0.0460	26.7448	6.280	15.9592	1.73	4.76092
24	1.615	-4.1635	0.0462	26.7072	6.829	16.6871	1.89	5.52924
25	0.098	20.1755	0.0691	23.2104	7.693	17.7219	1.41	2.98438
26	0.117	18.6363	0.0810	21.8303	9.184	19.2606	1.44	3.16725
27	0.218	13.2309	0.0940	20.5374	9.263	19.3350	1.40	2.92256

(with average of three set of replica)

## IV. RESULT AND DISCUSSION

In regression analysis, an equation consisting of values of a dependent response variables and one or more independent variables is derived for each quality characteristics. The dependent variables is modeled as a function of the independent terms and error functions. A linear regression equation is fitted by conducting analysis on the experimental data [13]. The regression equation helps to estimate the variables so as to give best fit of the output data.

### 4.1 Regression analysis

Regression equations are found out using software for statistical analysis called MINITAB 15. Regression equation helps to get the relation between different response variables and the input parameters. The software required the input conditions and the observations of the experiments which develops regression equation for each desired output. The regression equations obtained based on the experimental runs are as shown.

$$R_a = 2.73 - 0.00194 * \text{Concentration} - 0.0068 * \text{Temperature} + 0.0028 * \text{Time} \quad (1)$$

$$\text{MRR} = - 6.26 + 0.00673 * \text{Concentration} + 0.0677 * \text{Temperature} + 0.103 * \text{Time} \quad (2)$$

$$Uc = -0.0375 + 0.000071 * Concentration + 0.000657 * Temperature + 0.000326 * Time \tag{3}$$

$$EF = 0.951 - 0.000128 * Concentration - 0.00261 * Temperature + 0.0169 * Time \tag{4}$$

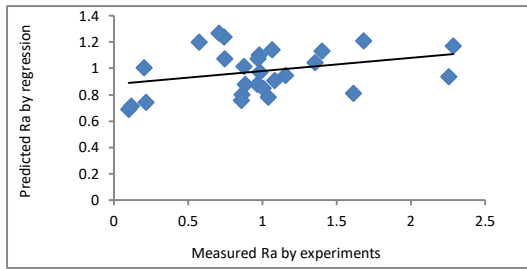


**Fig. 5 Comparison of experimental and regression model based prediction of Surface roughness (R<sup>2</sup>=0.67)**

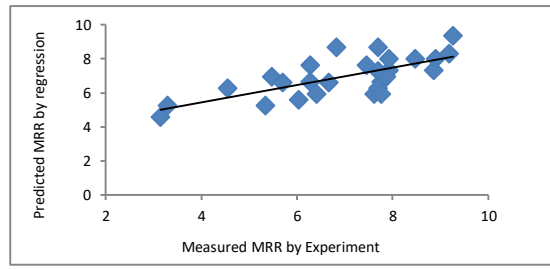


**Fig. 6 Comparison of experimental and regression model based prediction of Material Removal Rate (R<sup>2</sup>=0.92)**

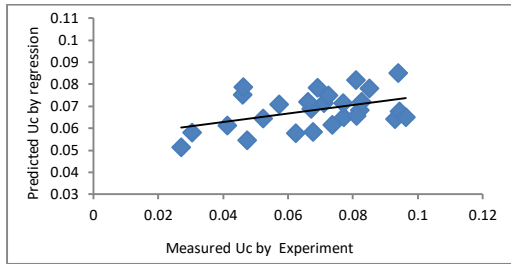


**Fig. 7 Comparison of Experimental and regression model based prediction of Undercut (R<sup>2</sup>=0.62)**

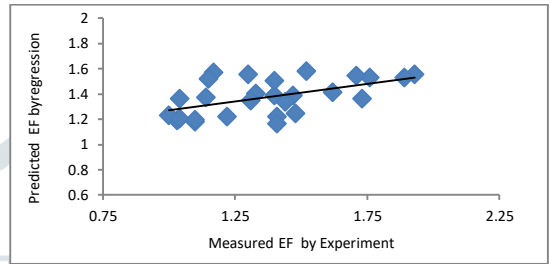


**Fig. 8 Comparison of Experimental and regression model based prediction of Etch Factor (R<sup>2</sup>=0.71)**

A comparison of the experimental and predicted Surface roughness (Ra), Material Removal Rate (MRR), Undercut (Uc) and Etch Factor (EF) obtained by equ.1, equ.2, equ.3 and equ.4 for all the 27 experimental runs are shown in Figure 5, Figure 6, Figure 7 and Figure 8. An excellent agreement is observed between the model predicted by regression and experimental value indicates the consistency of data (R<sup>2</sup> for Ra=0.67, R<sup>2</sup> for MRR=0.92, R<sup>2</sup> for Uc=0.62 and R<sup>2</sup> for EF=0.71). In the present study, a simple linear equation is able to successfully model the response values within the error range of 0 to 10%. The higher values are attributed to the likely presence of interactions amongst the three etching parameters but are limited to a few cases only. The same may not true beyond the range of parameters for a larger set of parameters and particularly where a non-linear relationship between the process parameters and response values may exist. [14].

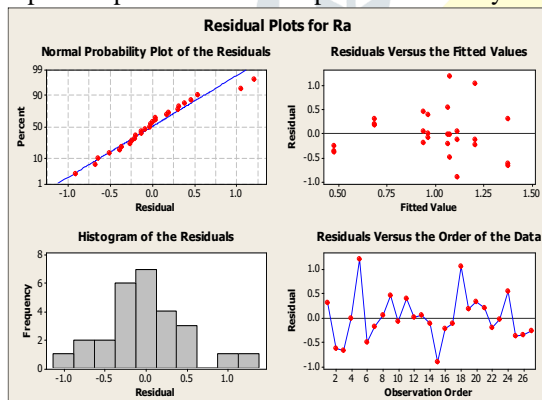


**Fig.9. Residual plot for Ra showing a) Normal probability plot b) Residual Vs scattered value c) Residual Vs fitted values d) plot for observation order.**

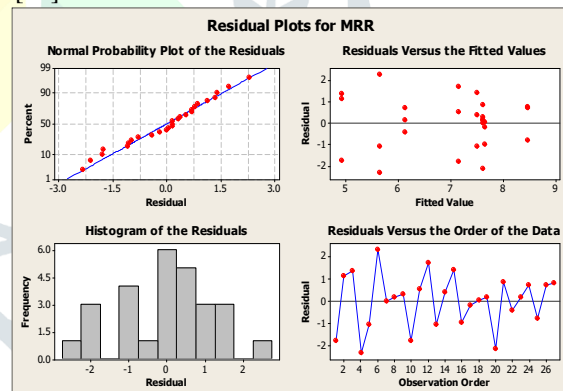


**Fig.10 Residual plot for MRR showing a) Normal probability plot b) Residual Vs scattered value c) Residual Vs fitted values d) plot for observation order.**

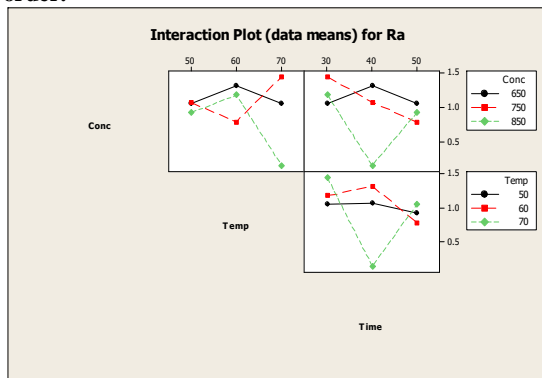


**Fig.11 Interaction plot for data means for Ra**

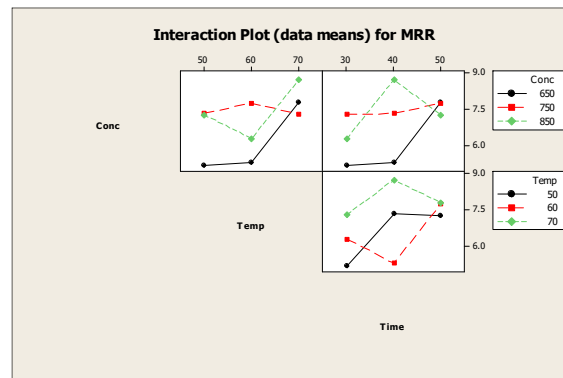


**Fig.12. Interaction plot for data means for MRR**

The distribution in Figure 9 and Figure 10 shows that the error normality assumption is valid. Figures give the plot of the residuals in time order of data collection. These graphs help to check the independence assumption on the residuals. It is desired that the residual plot should contain no apparent patterns. Figure 9 and 10 also shows residual plot & histogram for residual versus fitted values. The structure less distribution of dots above and below the abscissa (fitted values) shows that the errors are independently distributed and the variance is constant. It is concluded that the assumption of constant variance of residuals is satisfied. Confidence level is chosen to be 95% in this case. So the P- value which are less than 0.05 indicate that null hypothesis should be rejected, and thus the effect of the respective factor is significant.

**4.2 Analysis of Variance table for regression analysis**

Table 3. ANOVA Table for regression analysis

Source	D F	SS	MS	F	P
Regression	3	1.1705	0.3902	1.37	0.277
Residual Error	2	6.5449	0.2846		
Total	6	7.7154			

Table 4. Coefficient of regression analysis

Predictor	DF	SS Coef	T	p
Constant	3.454	1.312	2.63	0.015
Conc.	-	0.001257	-	0.137
Temp.	-0.00676	0.01257	-	0.596
Time	-0.01517	0.01257	-	0.240

The variance ratio denoted by F in ANOVA tables, is the ratio of the mean square due to a factor and the error means square. In this robust design F ratio can be used for qualitative understanding of the relative factor effects. A large value of F means that the effect of that factor is large compared to the error variance. Figure 11 and Figure 12, shows the interaction of machining parameters i.e. time of etching, temperature of etching and concentration of etchant on responses viz. Ra, MRR, EF and Uc. It is concluded that the assumption of constant variance of residuals is satisfied. Confidence level is chosen to be 95% in this case. So the p values which are less than 0.05 indicate that null hypothesis should be rejected, and thus the effect of the respective factor is significant. The variance ratio denoted by F in ANOVA Tables (shown in Table 3 and Table 4). The feasibility of developed model is checked by finding the percentage error between the experimental value and regression analysis ( shown in Table 5).

**Table 5** Validation of regression results with experimental results for MRR (mm<sup>3</sup>/min)

Ex · No	Experimental Value	Regression analysis (R <sup>2</sup> = 0.92 )			Exp No.	Experimental Value	Regression analysis (R <sup>2</sup> = 0.92 )		
		Predicted Value	Error	Percentage Error			Predicted Value	Error	Percentage Error
1	3.140	4.5895	1.4495	4.0571	14	7.879	6.9695	0.9095	1.1398
2	6.044	5.6195	0.4245	0.7876	15	8.910	7.9995	0.9105	1.2663
3	6.280	6.6495	0.3695	0.6856	16	6.672	6.6165	0.0555	0.0696
4	3.297	5.2665	1.9695	5.5126	17	7.457	7.6465	0.1895	0.2375
5	4.553	6.2965	1.7435	3.2350	18	7.693	8.6765	0.9835	1.2325
6	7.928	7.3265	0.6015	0.7587	19	7.771	5.9355	1.8355	2.9783
7	7.614	5.9435	1.6705	2.1940	20	5.479	6.9655	1.4865	2.4120
8	7.771	6.6735	1.0975	1.3754	21	8.478	7.9955	0.4825	0.6047
9	7.928	8.0035	0.0755	0.0946	22	5.700	6.6125	0.9125	1.4806
10	5.338	5.2625	0.0755	0.1414	23	6.280	7.6425	1.3625	1.7075
11	7.693	6.2925	1.4005	1.8205	24	6.829	8.625	1.796	2.3102
12	8.870	7.3225	1.5475	1.9393	25	7.693	7.2895	0.4035	0.5057
13	6.410	5.9395	0.4705	0.7634	26	9.184	8.3195	0.8645	1.0834
					27	9.263	9.3495	0.0865	0.1084

## V. Conclusion

One of the probable outcome of this study is development of Regression models for prediction of response parameters like, Surface roughness ( $R_a$ ), Material Removal Rate (MRR), Undercut (Uc) and Etch factor (EF) in PCM of SS-304. A good agreement of regression and experimental values is obtained with  $R^2$  values as 0.67, 0.92, 0.62 and 0.71 for  $R_a$ , MRR, Uc and EF respectively. A good performance of regression is achieved with by evaluating coefficient of determination ( $R^2$ ) between the predicted and experimented values. The experimental results after Design of Experiments with  $L_{27}$  orthogonal array are compared with the regression results. It is observed that percentage error in experimental and predicted results of regression are within the limit of 0 to 10% for most of results. Regression is used as an effective tool to map and model the PCM process parameters with predominant machining parameters like  $R_a$ , MRR, Uc and EF. The results show that regression model is used easily for the production of response parameters while PCM of SS-304 with time of etching, temperature of etchant and concentration of etchant as machining parameters. Regression modeling could prove to be a valuable approach for PCM companies to save and effort spend to correctly predict the responses in process.

## References

1. Cakir, O. 2005. Chemical etching of Cu-ETP copper. *Journal of Material Processing Technology*, 5: 275-279.
2. Allen, D. 2008. Photochemical Machining (PCM) of aluminum and its Alloys. *Competitive Manufacturing, Proc. of the 2<sup>nd</sup> Int. & 23<sup>rd</sup> AIMTDR Conf.*, Chennai, India. 37-44.
3. Tehrani, A. Fadaei, I. 2004. A new etchant chemical machining of St.304. *Journal of Material Processing Technology*, 149:404-408. doi:10.1016/j.matprotec.2004.02.055.
4. David, M. Heather J. 2004. Characterization of aqueous ferric chloride etchants used in industrial photochemical machining. *Journal of Material Processing Technology*, 149:238-245, doi:10.1016/j.matprotec.2004.02.44.
5. Cakir, O. 2008. Chemical etching of aluminum', *Journal of Material Processing Technology*, 199:337-340. doi: 10.1016/j.matprotec.2007.08.012.
6. Allen, D. Leong, T. 1999. Increasing utilization efficiency of ferric chloride etchant in industrial photochemical machining, *J. Environ. Monit.* 1:103-108.
7. Wangikar, S. Potawari, P. Mishra R. 2016. Effect of process parameters and optimization for Photochemical Machining of Brass and German silver. *Materials and Manufacturing Process*, 32:1747-1455, doi: 10.1080/10426914.2017.1317786.
8. Misal, N. Saraf, A. Sadaiah, M. 2017. Experimental investigation of surface topology in photochemical machining of Inconel 718. *Materials and Manufacturing Process*, doi.org/10.1080/10426914.2017.1317786.
9. Wei, W. Di, Z. Allen, D. Almond, H. 2008. Non-traditional machining techniques for fabricating metal aerospace filters. *Chinese Journal of Aeronautics*, 21:441-447.
10. Agrawal, D. Kamble, D. 2014. Multi-objective optimization of photochemical machining process based grey relational analysis method. *Applied Mechanics and Materials*, Transtech publications. Switzerland, 612, pp.77-82. doi:10.4028/www.scientific.Net/AMM.612.77.
11. Saraf, A. Sadaiah. (2013). Application of artificial intelligence for the prediction of undercut in photochemical machining', *International journal of Mechatronics and Manufacturing systems*, 6:183-194.
12. Agrawal, D. Kamble, D. 2018. Optimization of photochemical machining process parameters for manufacturing microfluidic channel. *Materials and Manufacturing process*, <https://doi.org/10.1080/10426914.2018.1512115>.
13. Dave, H. Ravik, K. Harit K. 2010. Modeling of cutting forces as a function of cutting parameters in milling process using regression analysis and artificial neural network, *International journal of Machining and Machinability of Materials*. 8(1/2):198-208.
14. Shukla, M. Tambe P. 2010. Predictive modeling of surface roughness and kerf widths in abrasive water jet cutting of Kevlar composites using neural network. *International journal of Machining and Machinability of Materials*. 8 (1/2):226-244.